ADVANCES IN ATMOSPHERIC SCIENCES, VOL. 31, JULY 2014, 972–984

Eddy Kinetic Energy Study of the Snowstorm over Southern China in January 2008

ZUO Qunjie[1,2], GAO Shouting[*1,3], and LÜ Daren[2]

[1]*Laboratory of Cloud-Precipitation Physics and Severe Storms, Institute of Atmospheric Physics, Chinese Academy of Sciences, Beijing* 100029

[2]*Key Laboratory of Middle Atmosphere and Global Environment Observation, Institute of Atmospheric Physics, Chinese Academy of Sciences, Beijing* 100029

[3]*State Key Laboratory of Severe Weather, Chinese Academy of Meteorological Sciences, Beijing* 100081

(Received 11 June 2013; revised 10 September 2013; accepted 25 October 2013)

ABSTRACT

The energetics of the third stage of a snowstorm over China was analyzed using ECWMF data. The analysis of the energy budget for the Middle East trough and the western Pacific trough that developed toward China on 25–28 January 2008 showed the advection of the geopotential by the ageostrophic wind to be both a crucial source and the primary sink of the eddy kinetic energy centers associated with the troughs. The magnitudes of the energy conversion terms, interaction kinetic energy conversion and baroclinic conversion, were too small to explain the development of the energy centers and the jet streaks. The energy centers gained energy at their entrance regions via the convergence of the ageostrophic geopotential fluxes, and then lost energy at their exit regions by the same fluxes. At the entrance regions, the fluxes converged, increasing the geopotential gradient, which generated a stronger geostrophic wind and higher kinetic energy, resulting in an ascending motion in this area. When the troughs moved to China, the ascending motion caused by the convergence of the fluxes at entrance region intensified the snowstorms over central and southern China.

Key words: eddy kinetic energy, ageostrophic geopotential flux, snowstorms, jet streaks

Citation: Zuo, Q. J., S. T. Gao, and D. R. Lü, 2014: Eddy kinetic energy study of the snowstorm over southern China in January 2008. *Adv. Atmos. Sci.*, **31**(4), 972–984, doi: 10.1007/s00376-013-3122-z.

1. Introduction

From early January to early February 2008, China experienced long-lasting and extraordinary snowstorms. Low temperature, an excessive amount of snow and severe freezing rain over central and southern China caused deaths and severe damage to property. The snow and ice storms occurred in four episodes: 10–16, 18–22, 25–29 January, and 31 January –2 February (Sun and Zhao, 2010).

There have been numerous studies that relate tropospheric jet streams to the development of severe convective storms. The upper tropospheric jet stream advects cool and dry air in the upper and middle troposphere, which enhances upper-level divergence, and transports the sensible heat downstream from the convective region (Petterssen, 1956; Reiter, 1963; Ludlam, 1963; Newton, 1963, 1967; Palmén and Newton, 1969; Danielsen, 1974). Jet-stream-induced transverse circulations and their associated ascending motion can cause a wide range of convective storms. Uccellini and Kocin (1987) found that vertical motions enhanced by the ascending branches of the two jets over the northeast and the south-central United States contributed to heavy snowfall. Using a set of observations and numerical simulations, the dual jet stream pattern was found to play an important role in locally enhancing the vertical motion and precipitation rates (Velden and Mills, 1990; Crochet et al., 1990; Junker et al., 1990).

The subtropical jet stream was important to the development of the snowstorm over central and southern China in January 2008. When the Middle East jet streams strengthened and shifted southeastward, the westerlies over India and the southern Tibetan Plateau were enhanced (Wen et al., 2009; Zhou et al., 2009; Shi et al., 2010). During the same period, a deepening trough embedded in the southern branch of the westerlies, enhanced the water vapor transport from western Asia and the Bay of Bengal to China. The intensification and southeastward shift of the Middle East jet streams were accompanied by a decreasing temperature over most of China and wet conditions over southern China (Wen et al., 2009). In this paper, we focus on the factors that strengthened and shifted the subtropical jet streaks, and then affected the

* Corresponding author: GAO Shouting
Email: gst@mail.iap.ac.cn

ascending motion associated with the snowstorm over China in January 2008.

2. Data and method

Six-hourly ECMWF (European Centre for Medium-Range Weather Forecasts) Interim Re-analysis (ERA-Interim; Simmons et al., 2007) data (geopotential and wind speed) for January 2008 were used in our analysis. The horizontal resolution of the dataset is $1.5^\circ \times 1.5^\circ$ with 37 vertical pressure levels from 1000 to 1 hPa.

To study the development of jet streams over China during the third stage of the snowstorms, an eddy kinetic energy (EKE) tendency equation was used as a fundamental tool in this study.

Based on Murakami's (2011) work, the EKE (k') equation is given as

$$\frac{\partial k'}{\partial t} = -\boldsymbol{V}\cdot\nabla k' - \boldsymbol{V}_2'\cdot(\boldsymbol{V}'\cdot\nabla\overline{\boldsymbol{V}_2}) - \boldsymbol{V}'\cdot\nabla\phi' - \omega'\alpha' + \boldsymbol{V}_2'\cdot(\overline{\boldsymbol{V}'\cdot\nabla\boldsymbol{V}_2'}) + X\ , \quad (1)$$

where ϕ is geopotential, $k' = (u'^2 + v'^2)/2$, $\boldsymbol{V} = [u, v, \omega]^{\mathrm{T}}$ (superscript T denotes a vector transpose), $\boldsymbol{V}_2 = [u, v, 0]^{\mathrm{T}}$, $\alpha' = -\partial\phi'/\partial p$, (u, v) represents the zonal and meridional winds, $\omega(= dp/dt)$ is the vertical velocity, p is pressure (hPa), t is time, and ∇ is the three-dimensional gradient operator. The overline denotes the zonal mean, and the prime denotes small perturbations to a zonal mean flow.

The term on the left-hand side of Eq. (1) is the local tendency. The first term on the right-hand side (rhs) of (1) is the eddy kinetic energy advection by flow, which can be decomposed into the mean and eddy advections ($-\boldsymbol{V}\cdot\nabla k' = -\overline{\boldsymbol{V}}\cdot\nabla k' - \boldsymbol{V}'\cdot\nabla k'$). The second term on the rhs of Eq. (1) is interpreted as an energy conversion rate between the interaction kinetic energy $(uu' + vv')$ and the eddy kinetic energy, when averaged over the zone (Orlanski and Katzfey, 1991; Murakami, 2011). The third term is the generation of the eddy kinetic energy, associated with the pressure gradient and eddies. Similar to Orlanski and Katzfey's (1991) work, this term can be rewritten as

$$-\boldsymbol{V}'\cdot\nabla\phi' = -\nabla\cdot(\boldsymbol{V}_{\mathrm{a}}'\phi')\ , \quad (2)$$

where the subscript a indicates ageostrophic and $\boldsymbol{V}_{\mathrm{a}} = [u_{\mathrm{a}}, v_{\mathrm{a}}, \omega]^{\mathrm{T}}$. This term represents the divergence of a radiative energy flux. The fourth term on the rhs of Eq. (1) is the baroclinic conversion of the eddy available potential energy. When $\omega'\alpha'$ is negative, the eddy available potential energy is converted to eddy kinetic energy. The fifth term on the rhs of Eq. (1) is the energy conversion by Reynolds stresses and is zero in the zonal mean sense. X represents the horizontal frictional sink.

3. The variation of eddy kinetic energy and jet streams in the subtropics

The evolutions of the 250-hPa eddy kinetic energy and jet streams from 25 to 28 January 2008 are shown in Fig. 1.

On 25 January 2008, there were two obvious troughs: one over the Middle East with a northeast–southwest orientation, and the other over the western Pacific with a northwest–southeast orientation. The eddy kinetic energy center was located upstream (western side) or downstream (eastern side) of each trough (Fig. 1a). In Fig. 1, the letters A to F indicate the eddy kinetic energy centers: A is around (50°N, 80°E), B is around (30°N, 65°E), C is around (30°N, 80°E), D is around (35°N, 140°E), E is around (55°N, 120°E), and F is around (50°N, 170°E). These letters also indicate the centers of the jet streams. The first four energy centers are associated with the maxima of the zonal wind, and the energy centers *E* and *F* are associated with the maxima of the meridional wind (Fig. 1a).

From 25 to 26 January 2008, energy center A in the midlatitudes and energy center B on the upstream of the deepening Middle East trough decreased, while on the downstream of the trough energy center C increased (Figs. 1a and b). During the same period, energy center D on the upstream of the western Pacific trough and energy center E in the midlatitudes decreased, and energy center F on the downstream of the western Pacific trough increased (Figs. 1a and b). From 26 to 27 January 2008, the Middle East trough and the accompanying energy centers moved eastward about 10° (Figs. 1b and c). Energy center B increased and energy center C remained the same (Figs. 1b and c). During this period, energy center D decayed and energy center F split into two weak centers (Figs. 1b and c). From 27 to 28 January 2008, the Middle East trough moved continually eastward, and energy centers C and D combined and strengthened on the downstream of the trough. This new energy center around (35°N, 120°E) is indicated by the letter G on 28 January 2008 (Figs. 1c and d). During the same period, two energy centers on the downstream of the western Pacific trough combined around (45°N, 180°E), which is also indicated by the letter F (Figs. 1c and d).

The longitude–height cross sections of the eddy kinetic energy and zonal wind averaged over 20°–35°N and 25°–45°N are not shown here. The zonal wind maximum centers corresponded to the eddy kinetic energy centers from 25 to 28 January 2008.

The energy centers in the subtropics were actually the signature of the well-known "jet streams" and the development of the energy center can be considered as the development of the jet streams (Uccellini and Johnson, 1979; Bluestein, 1993; Orlanski and Sheldon, 1995). In the next section, the eddy kinetic energy equation is used to study the variation of the energy centers and also the variation of the jet streams over southern China.

4. Eddy kinetic energy budget

To better understand the conversion, transport, sources and sinks associated with the eddy kinetic energy patterns during the third stage of the snowstorm over southern China in January 2008 shown in Fig. 1, the eddy kinetic energy budget is analyzed by applying Eq. (1).

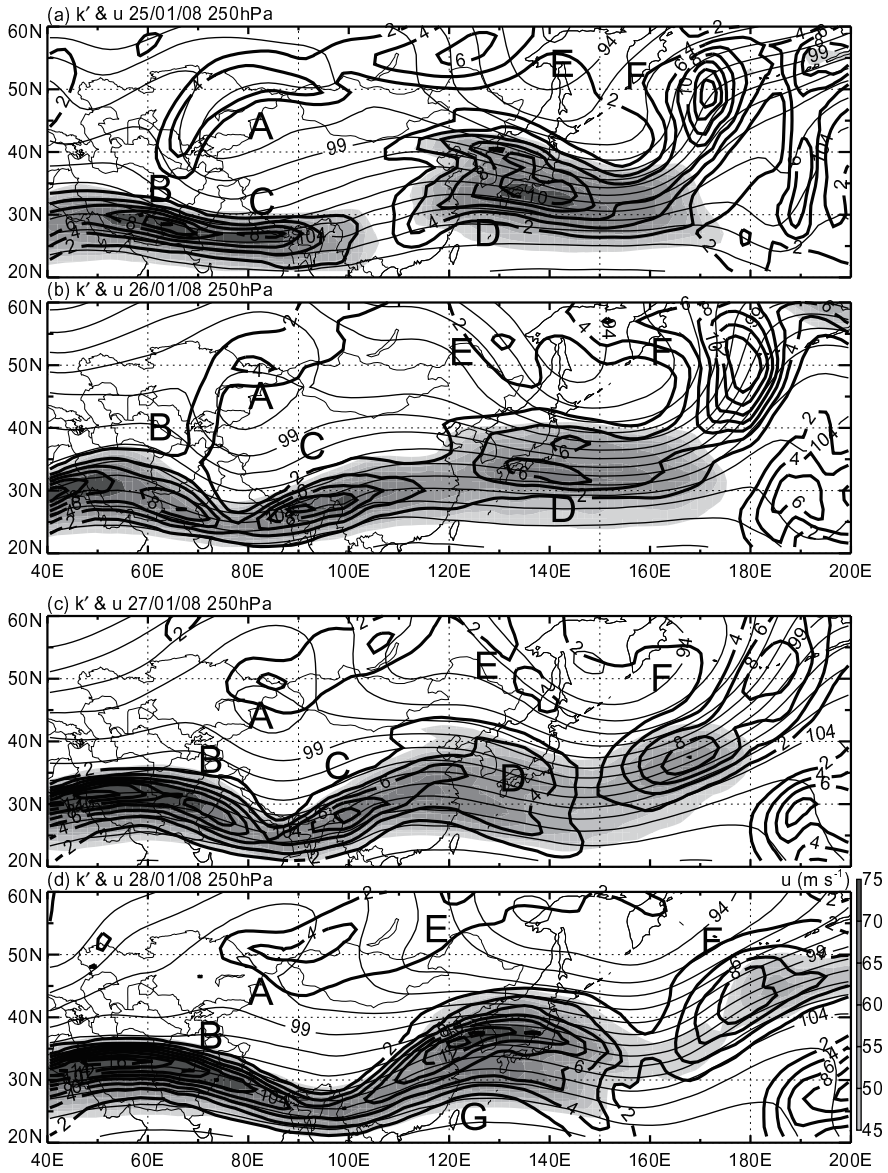

Fig. 1. The 250-hPa eddy kinetic energy (thick solid lines, interval: 2×10^2 m^2 s^{-2}), geopotential (thin solid lines, 1×10^2 m^2 s^{-2}), and zonal wind (shaded, $\geqslant 45$ m s^{-1}, interval is 5 m s^{-1}) on (a) 25, (b) 26, (c) 27, and (d) 28 January 2008. The upper case letters indicate the positions of kinetic energy centers.

The advection of the eddy kinetic energy by wind is not shown here, but the horizontal flux of the eddy kinetic energy ($\boldsymbol{V}_2 k'$) at 250 hPa from 25 to 28 January 2008 is shown in Fig. 2. The maxima of the flux were located in the eddy kinetic energy centers with the direction from the upstream to the downstream of each energy center (Fig. 2). Although the advection was larger than the other terms of Eq. (1), its function was mainly to redistribute the eddy kinetic energy from the upstream to the downstream of the energy center not between the energy centers (this can also be found in the latitude–height cross sections, which are not shown here). It is important to point out that this process could not increase the geopotential gradient or generate a new energy center, and its contribution to the eddy kinetic energy is largely cancelled when integrated over a volume including the whole disturbance.

The conversion between the eddy kinetic energy and the interaction kinetic energy at 250 hPa is shown in Fig. 3. On the upstream of the Middle East trough, the interaction kinetic energy was converted to eddy kinetic energy in energy center B, which increased energy center B from 25 to 28 January 2008 at 250 hPa (Fig. 3). On the downstream of this trough, the eddy energy was mainly converted to interaction energy in energy center C at 250 hPa during this

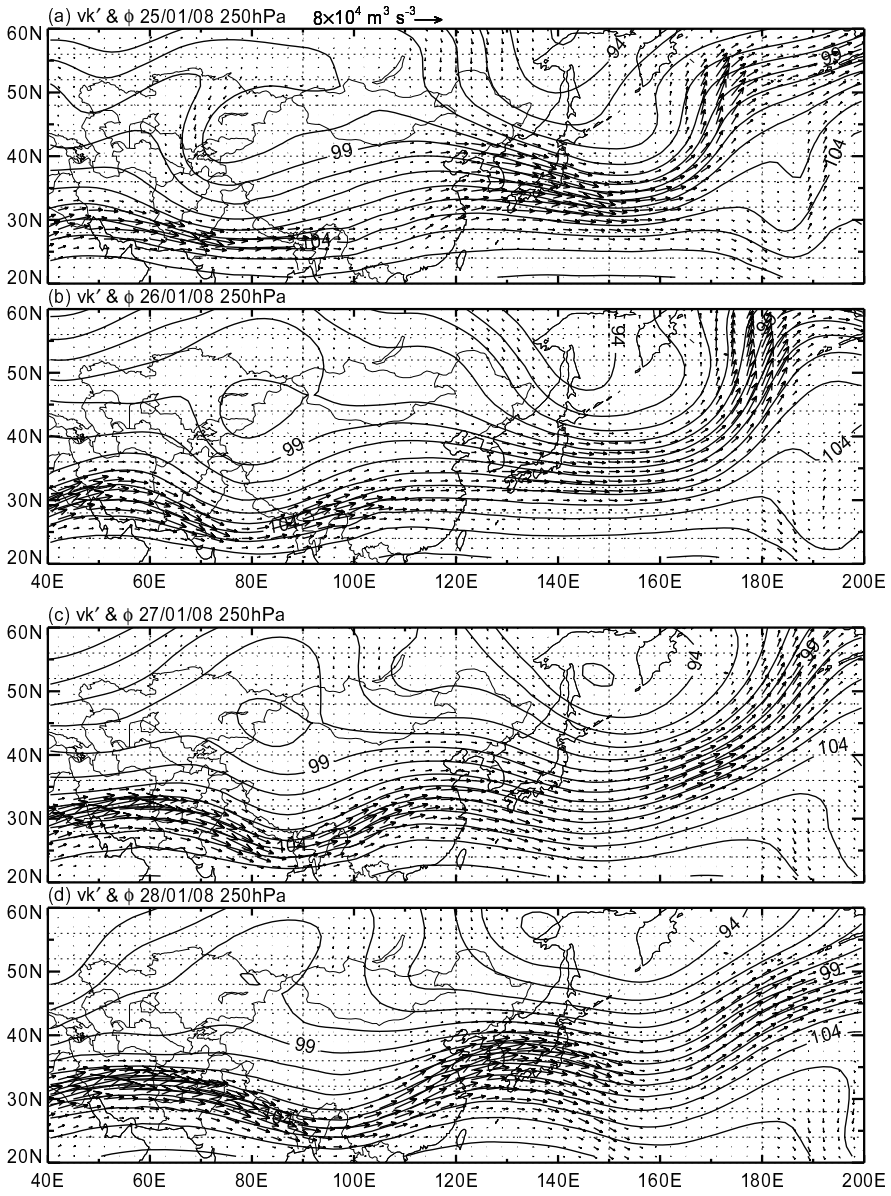

Fig. 2. The 250-hPa geopotential (thin solid lines, 1×10^2 m^2 s^{-2}) and eddy kinetic energy flux vectors (units: 8×10^4 m^3 s^{-3}) on (a) 25, (b) 26, (c) 27, and (d) 28 January 2008.

period, which decreased energy center C (G on 28 January) (Fig. 3). With the eastward movement of the energy center, the conversion moved eastward. The conversion associated with the western Pacific trough was less than in the Middle East trough (Fig. 3).

The longitude–height cross sections of the conversion between the interaction kinetic energy and the eddy kinetic energy and zonal wind averaged over 20°–35°N and 25°–45°N are shown in Fig. 4. On the upstream of the Middle East trough (Figs. 4a–d), the conversion from interaction kinetic energy to eddy kinetic energy increased energy center B. On the downstream of the trough (Figs. 4a–d), the conversion from eddy kinetic energy to interaction kinetic energy decreased energy center C (G on 28 January). During these four days, energy center B (C) decreased (increased), while the conversion contributed to strengthen (weaken) the energy center, which indicates that the net tendency of the centers were determined more by the remaining terms in Eq. (1). On the downstream of the western Pacific trough, the conversion was less than in the Middle East trough (Figs. 4e–h).

The eddy kinetic generation ($-\boldsymbol{V}' \cdot \nabla\phi'$) and the baroclinic conversion between the eddy available potential energy and the eddy kinetic energy ($\omega'\alpha'$) play significant roles in the net growth or decay of the eddy kinetic energy.

The baroclinic conversion at 250 hPa is shown in Fig. 5. The conversion decreased energy center B on the upstream

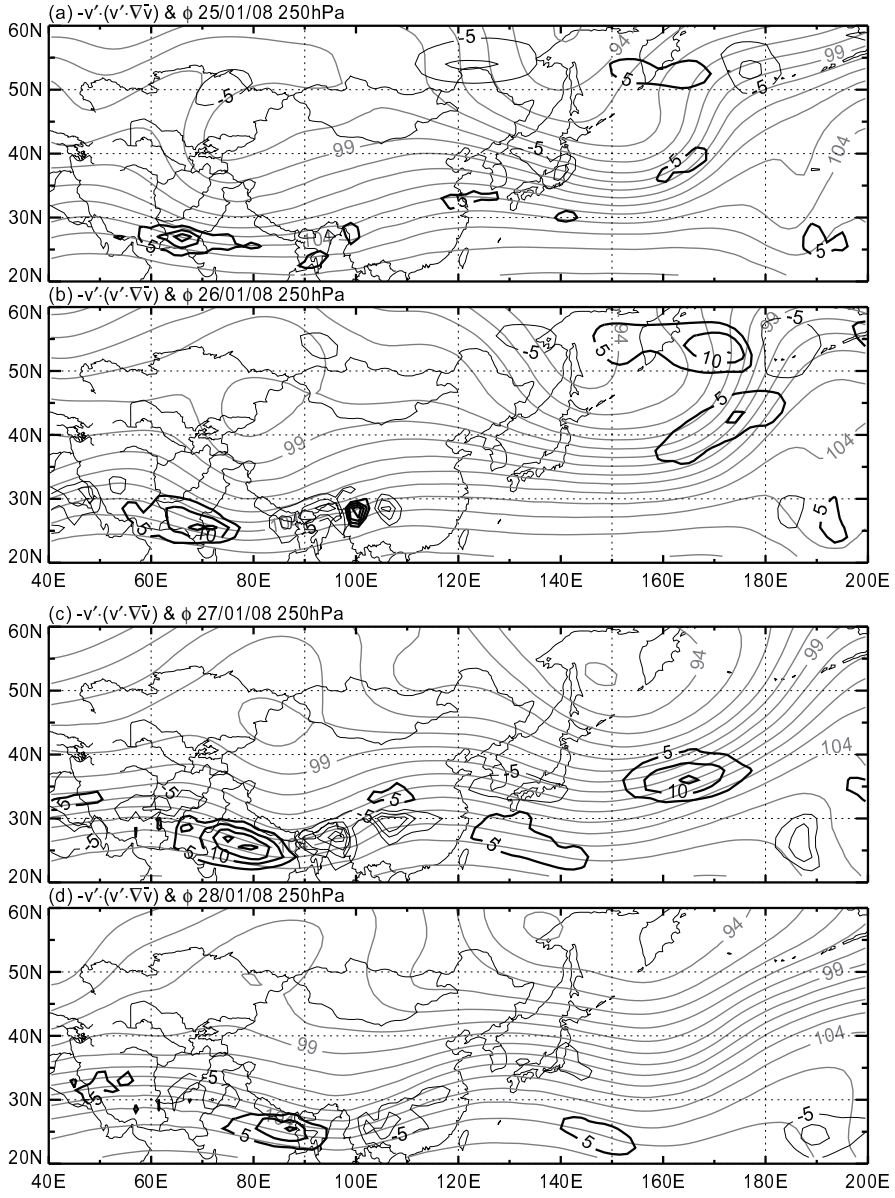

Fig. 3. The 250-hPa conversion between the interaction kinetic energy and the eddy kinetic energy (thick black solid lines: positive; thin black solid lines: negative; interval is 5×10^{-3} m^2 s^{-3}) and geopotential (thin gray lines, 1×10^2 m^2 s^{-2}) on (a) 25, (b) 26, (c) 27, and (d) 28 January 2008.

of the Middle East trough, and almost increased energy center C on the downstream of the trough from 25 to 28 January (Figs. 5a–d). On the western Pacific trough, the baroclinic conversion played little role in the variations of the eddy kinetic energy (Figs. 5a–d)

In the vertical section (Fig. 6), the negative conversion mainly appeared in the middle and upper troposphere. The negative conversion on the downstream of the trough indicated that ascending motion was active, which provided favorable conditions for the growth of the snowstorm over southern China.

The quantity $-\boldsymbol{V}' \cdot \nabla\phi'$ together with the vector of ageostrophic geopotential flux at 250 hPa is shown in Fig. 7. In this section, we mainly focus on the development of the downstream of the Middle East trough, i.e., energy center C or G, because this area of the trough played a crucial role in the snowstorm over southern China in January 2008.

The magnitude of this term is obviously more than those of the baroclinic conversion and the conversion between the eddy kinetic energy and the interaction kinetic energy. So, the variation of the energy centers or jet streaks was mainly decided by this term. On 25 January 2008, the fluxes diverged at the exit region of energy center A in the midlatitude and energy center B on the upstream of the Middle East trough,

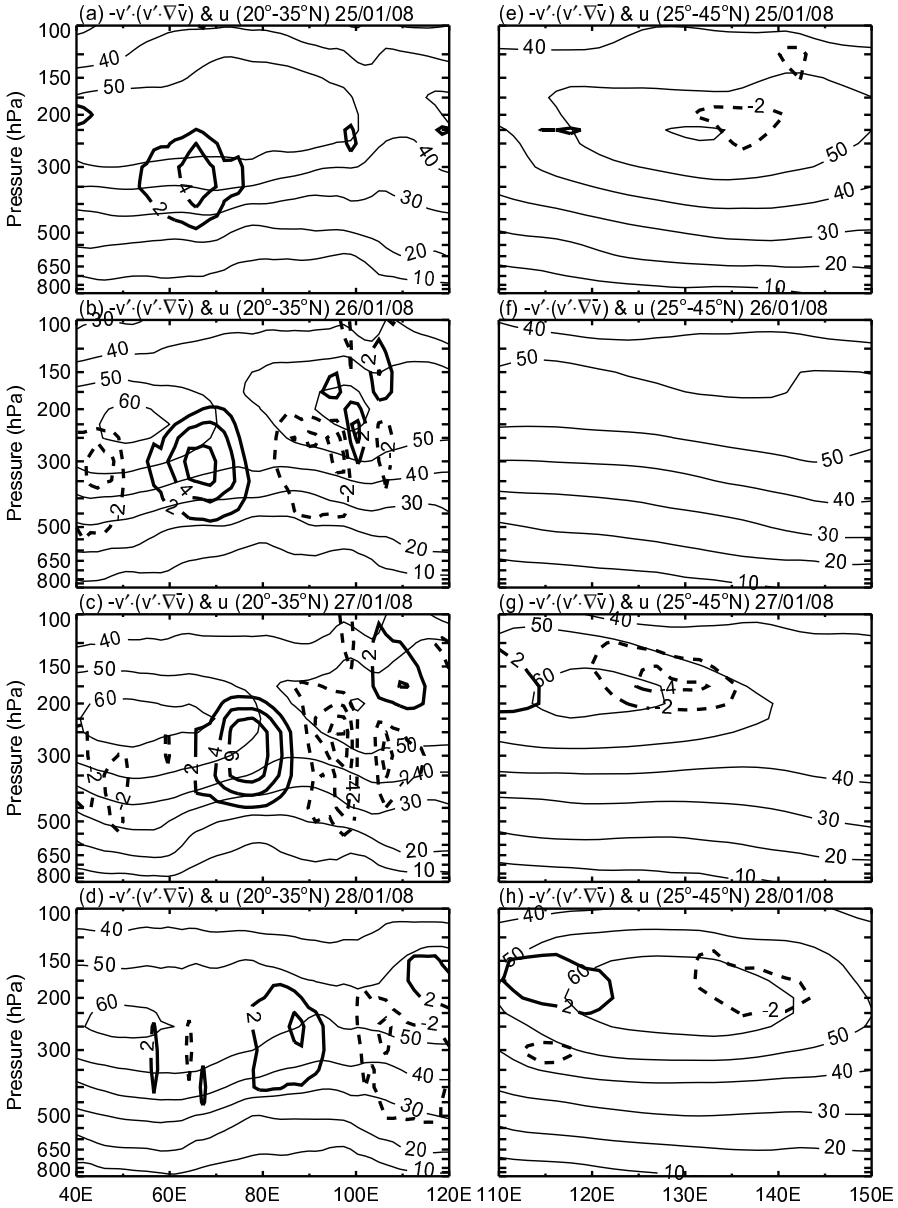

Fig. 4. Longitude–height cross sections of the conversion between the interaction kinetic energy and the eddy kinetic energy (thick solid lines: positive, thick dashed lines: negative; interval: 2×10^{-3} m^2 s^{-3}) and zonal wind (solid lines, interval: 10 m s^{-1}) averaged over 20°–35°N (left panels) and 25°–45°N (right panels) from 25 to 28 January 2008.

and they converged at the entrance region of energy center C on the downstream of this trough. The eddy kinetic energy was transported from energy centers A and B to energy center C via ageostrophic geopotential fluxes. These fluxes from different regions were deposited on the downstream of the trough, increasing the geopotential gradient and generating a stronger geopotential wind and higher eddy kinetic center C. Energy center B was compensated by the ageostrophic geopotential flux convergence at its entrance region from its upstream and by the conversion from interaction energy mentioned above in Fig. 3. Although energy center C obtained energy at its entrance region, it did not grow limitlessly. The energy was transported by the eddy kinetic energy flux itself ($\boldsymbol{V}_2 k'$) from the entrance region to the exit region of energy center C. It then lost energy primarily through the divergence of the ageostrophic geopotential flux, which transferred energy down to the tropic somewhere (Fig. 7a), and to a lesser extent through the conversion to interaction energy (Figs. 3a and 4a).

From 25 to 28 January 2008, energy center A decreased because it lost energy to energy center C. The decay of energy center B was slight relative to energy center A because of the

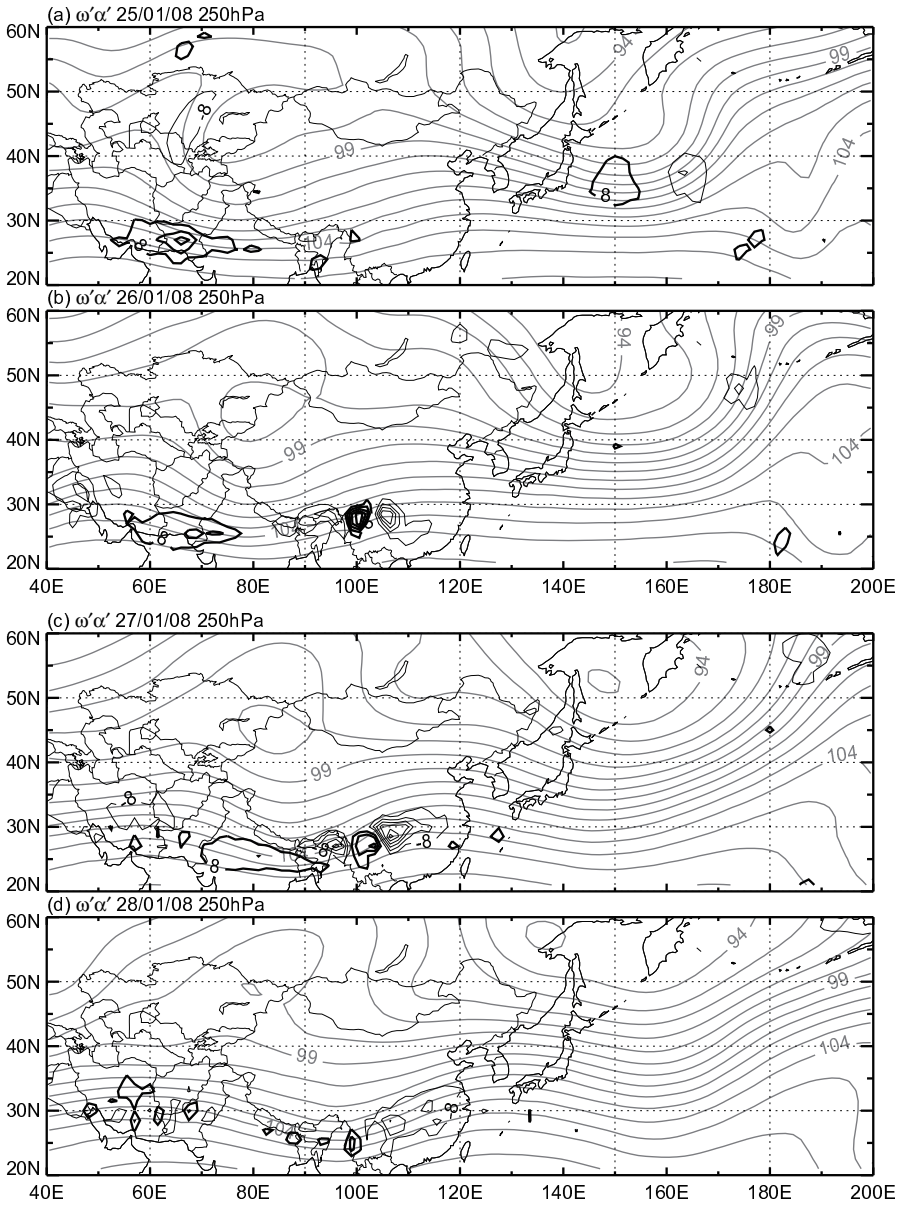

Fig. 5. The 250-hPa baroclinic conversion (thick black solid lines: positive; thin black solid lines: negative; interval is 8×10^{-3} m^2 s^{-3}) and geopotential (thin gray lines, 1×10^2 m^2 s^{-2}) on (a) 25, (b) 26, (c) 27, and (d) 28 January 2008.

energy compensation from its upstream by the ageostrophic geopotential flux (Fig. 7) and the conversion locally from the interaction energy (Figs. 3 and 4). Energy center C obtained energy from energy centers A and B from 25 to 27 January 2008 (Figs. 7a–c). With the movement of the Middle East trough and the variation of the western Pacific trough, energy centers C and D were combined as the energy center G over central China on 28 January 2008 (Fig. 7d).

We now focus on the development of energy center D at 250 hPa. On 25 January 2008, the ageostrophic geopotential fluxes converged at the entrance region of energy center D from energy center E and south of 20°N. Energy center D obtained energy from these two areas, and lost energy from its exit region to energy center F on the downstream of the western Pacific trough by the ageostrophic geopotential flux (Fig. 7a). On 26 January 2008, energy center D no longer obtained energy from the tropic (Fig. 7b), resulting in the decrease of the flux convergence at the entrance region from about 30 m^3 s^{-3} on 25 January 2008 (Fig. 7a) to 20 m^3 s^{-3} on 26 January 2008 (Fig. 7b). Simultaneously, the flux divergence at its exit region decreased from about 25 m^3 s^{-3} (Fig. 7a) to 10 m^3 s^{-3} (Fig. 7b). Consequently, the energy center decayed during this period (Figs. 1a and b). From 26 to 27 January 2008 at 250 hPa, the convergence of the

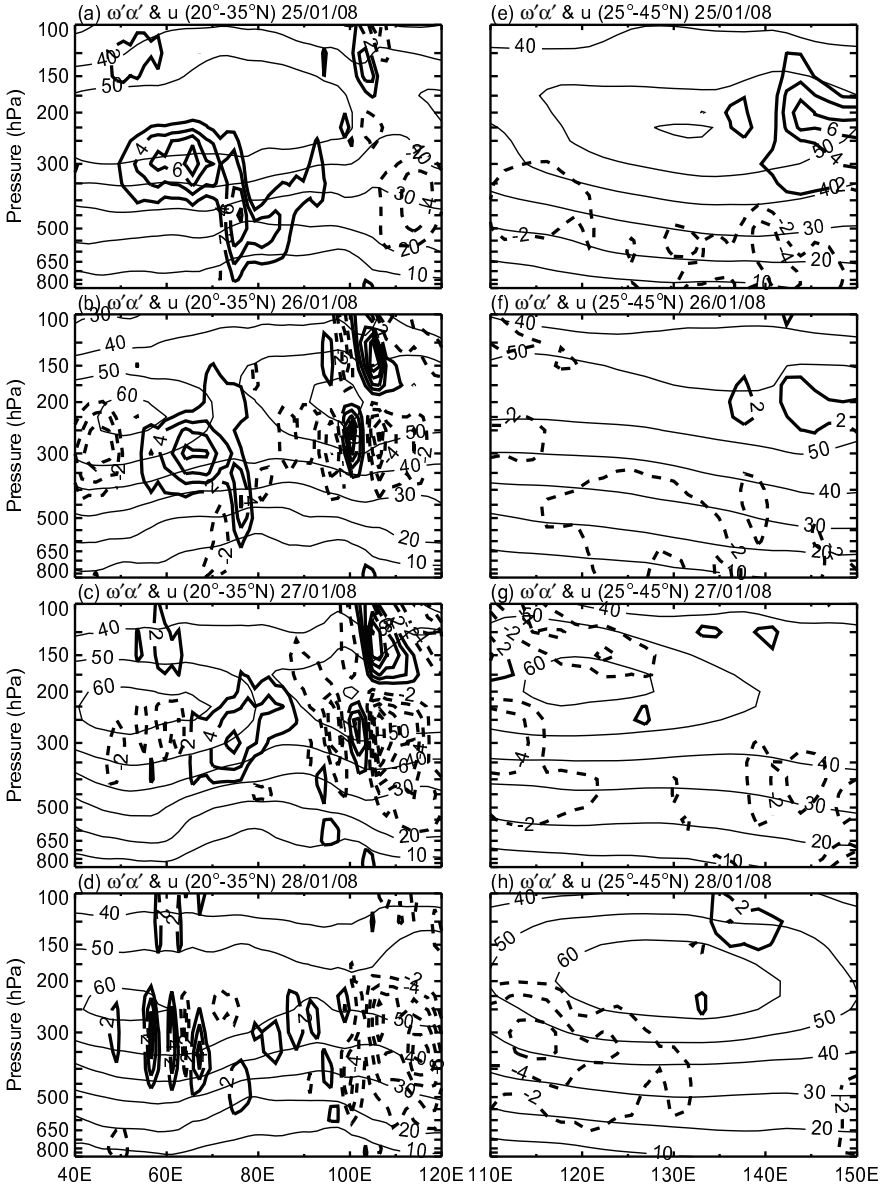

Fig. 6. Longitude–height cross sections of the baroclinic conversion (thick solid lines: positive, thick dashed lines: negative; interval: 2×10^{-3} m^2 s^{-3}) and zonal wind (solid lines, interval: 10 m s^{-1}) averaged over 20°–35°N (left panels) and 25°–45°N (right panels) from 25 to 28 January 2008.

ageostrophic geopotential flux decreased continually at its entrance region and moved northward from 35°N to 40°N, and the divergence increased at its exit region (Figs. 7b and c), resulting in its decay and northward movement (Figs. 1b and c). From 27 to 28 January, the energy centers C and D encountered and merged as energy center G over central and southern China at 250 hPa (Figs. 7c and d). Energy center D or G (on 28 January) mainly obtained energy from energy center E by the ageostrophic geopotential flux from 25 to 28 January (Fig. 7). The eddy kinetic energy was transported to central and southern China from the mid-high latitude via the ageostrophic geopotential flux (Fig. 7). These behaviors were similar to the southward propagation of the planetary wave (Zuo et al., 2013). The North Pacific cyclone was examined in terms of eddy energy and a phase-independent wave activity obtained by Takaya and Nakamura (2001). Contrasting these two diagnoses, there were minor differences during much of the initial evolution (Danielson et al., 2006). These indicated that $\boldsymbol{V}_{\rm a}' \cdot \phi'$ could be used to track a wave packet as it moved downstream not only in the mid-high latitudes, but also in the subtropics.

The longitude–height cross sections of the quantity

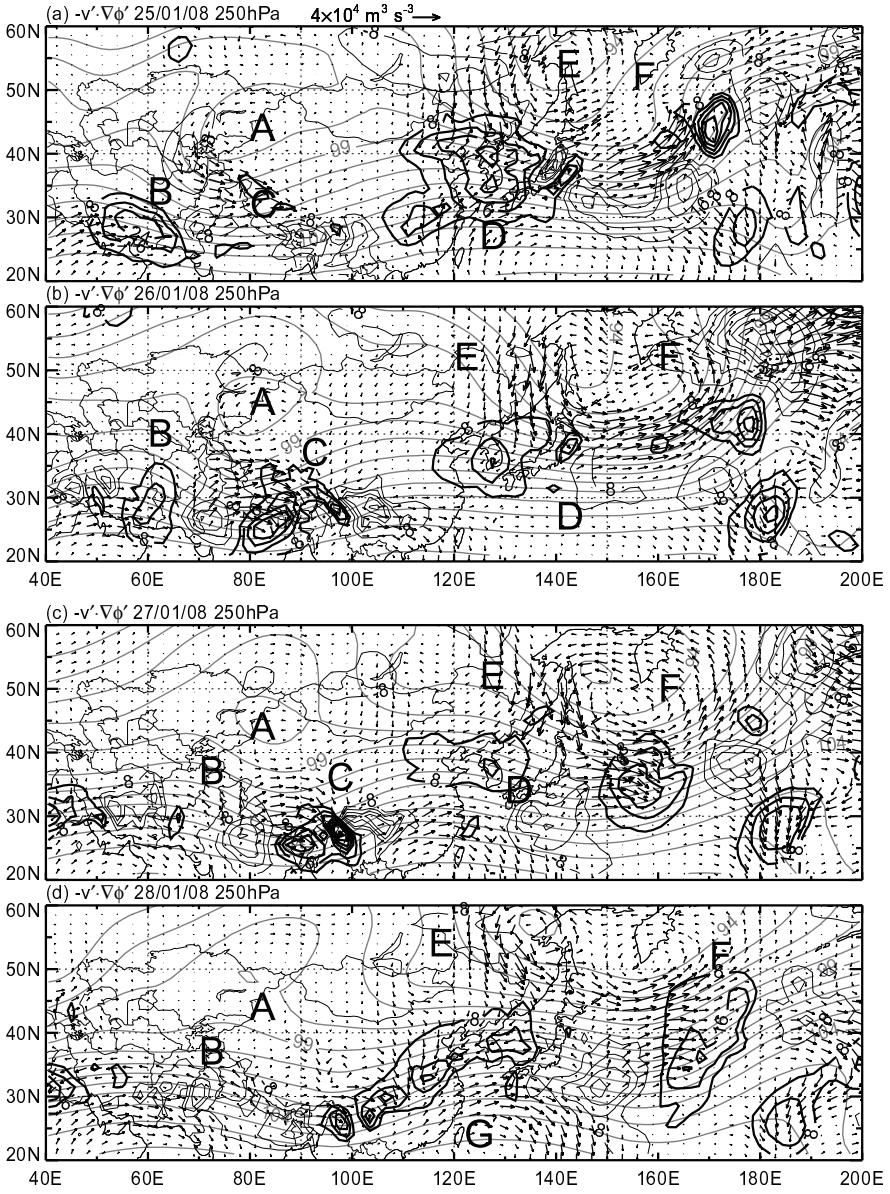

Fig. 7. The 250-hPa eddy advection of geopotential (thick black solid lines: positive; thin black solid lines: negative; interval is 8×10^{-3} m^2 s^{-3}), geopotential (thin gray lines, 1×10^2 m^2 s^{-2}), and ageostrophic geopotential eddy flux vectors (units: 4×10^4 m^3 s^{-3}) on (a) 25, (b) 26, (c) 27, and (d) 28 January 2008.

$-\boldsymbol{V}' \cdot \nabla\phi'$ averaged over 20°–35°N and 25°–45°N are shown in Fig. 8, which demonstrates the zonal and vertical transport of kinetic energy; and the latitude–height cross sections of $-\boldsymbol{V}' \cdot \nabla\phi'$ over 60°–90°E and 100°–150°E are shown in Fig. 9, which demonstrates the meridional and vertical transport of the kinetic energy. The characteristics of convergence at the entrance region of energy center C and the divergence at the exit region of energy center B can also be seen in Figs. 8 and 9. The ageostrophic geopotential flux transported energy from the downside of B's exit region up to C's entrance region and converged there (Figs. 8b and c). Note that energy center C also transported energy internally from its exit region down to its entrance region by the ageostrophic geopotential flux (Figs. 8b and c). Energy center D obviously obtained energy from the surface before it combined with energy center C (Figs. 8e–f). After energy center G appeared, the energy transport from the surface decreased (Fig. 8h). Energy centers C and D or G not only gained energy from its upstream and surface but also from the mid-high latitude and tropic in the upper troposphere (Fig. 9).

The formation of the energy centers can be considered as the manner in which the jet streaks were generated. The variation of the upper jet streaks and the trough could have caused the development of vertical motion. From 25 to 26

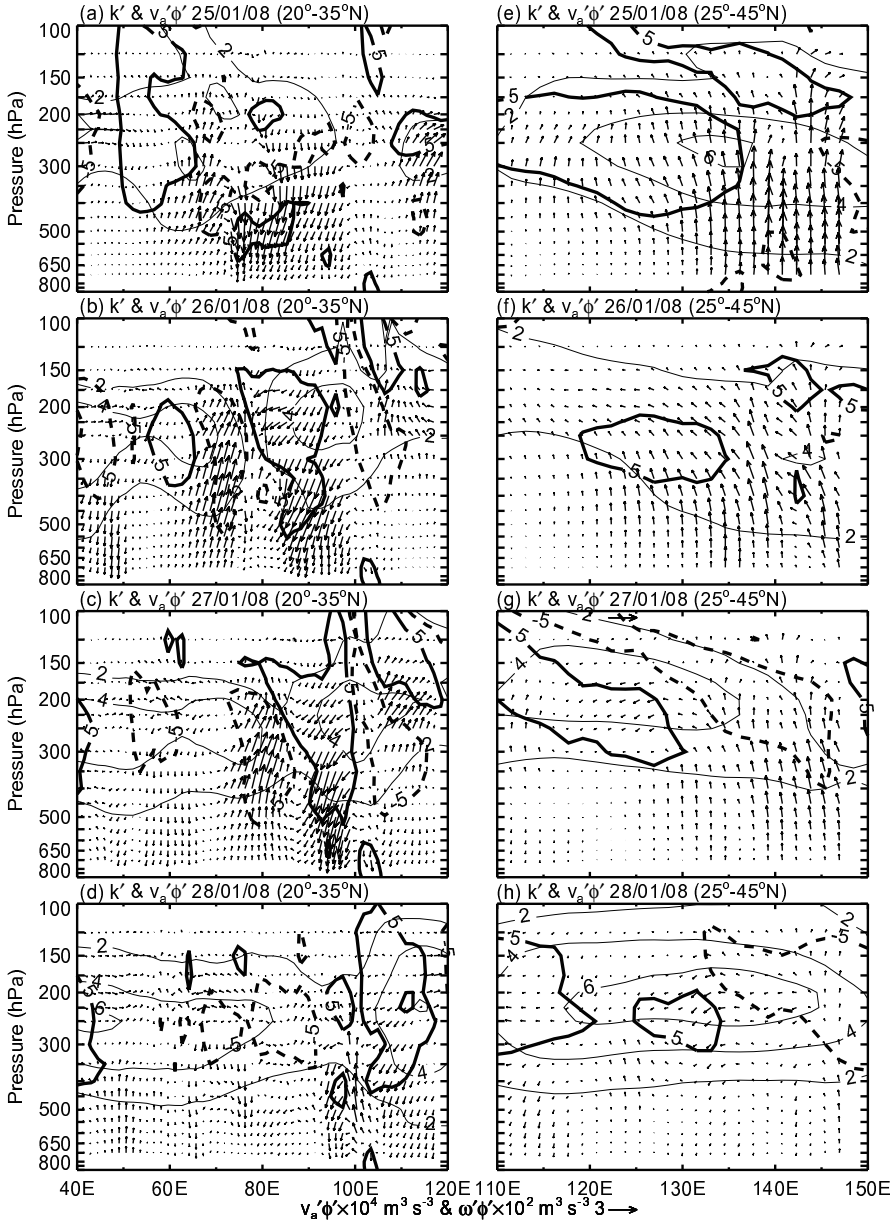

Fig. 8. Longitude–height cross sections of eddy advection of geopotential (thick solid lines: 5×10^{-3} m^2 s^{-3}, thick dashed lines: -5×10^{-3} m^2 s^{-3}), eddy kinetic energy (thin solid lines, interval: 2×10^2 m^2 s^{-2}), and ageostrophic geopotential eddy flux vectors averaged over 20°–35°N (left panels) and 25°–45°N (right panels) from 25 to 28 January 2008.

January, the ascending motion decreased over southern China (Figs. 10a and b), since energy center D or the East Asian jet decreased. With the eastward movement of energy center C and the northward movement of energy center D from 26 to 27 January 2008, a tilting jet controlled central China (Figs. 1b and c), resulting in the ascending motion increasing and moving northward (Figs. 10b and c). When energy center G appeared over China, the tilting jet moved southward and strengthened (Fig. 1d), leading to the ascending motion increasing and moving southward (Fig. 10d). Ascending motion played a crucial role in the snowstorm over central and southern China in January 2008 and appeared primarily at the entrance region of the jet streaks or energy centers C and D or G (Fig. 10). Since this was an area in which the ageostrophic geopotential flux converged, the geopotential height gradient increased and therefore strengthened the jet streaks and kinetic energy, thereby enhancing the ascending motion over central and southern China in January 2008, adding to energy centers C and D or G via baroclinic conversion. So the vertical motion over central and southern China was affected not only by its upstream (energy centers B and C) and downstream (energy center D) systems but by the midlatitude sys-

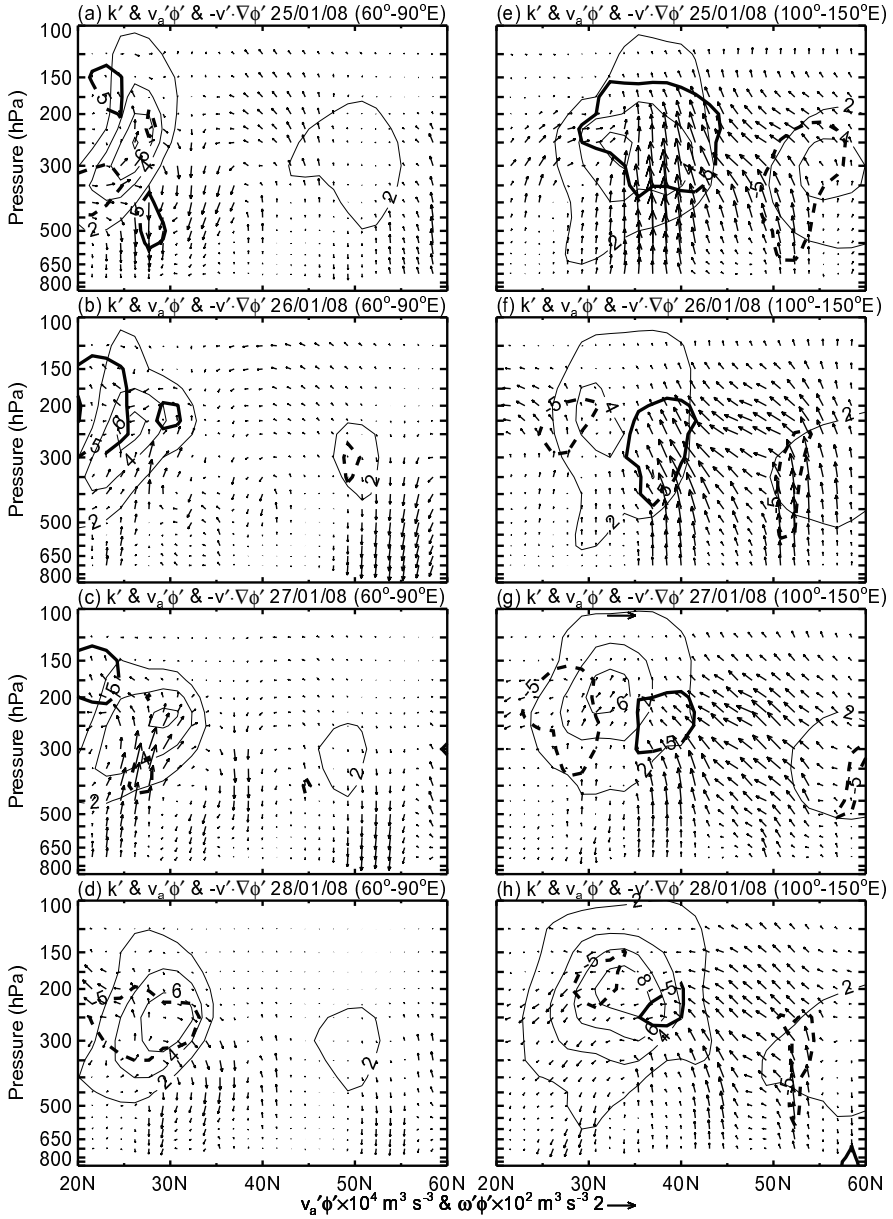

Fig. 9. Latitude–height cross sections of eddy advection of geopotential (thick solid lines: 5×10^{-3} m^2 s^{-3}, thick dash lines: -5×10^{-3} m^2 s^{-3}), eddy kinetic energy (thin solid lines, interval: 2×10^2 m^2 s^{-2}), and ageostrophic geopotential eddy flux vectors averaged over 60°–90°E (left panels) and 100°–150°E (right panels) from 25 to 28 January 2008.

tems (energy centers A and E) and somewhere in the tropic via ageostrophic geopotential fluxes.

5. Conclusions

The evolution of EKE and jet streaks during the third stage of the snowstorms over China in January 2008 was investigated using the ECMWF data. The energy center, jet streaks and associated Middle East trough and western Pacific trough displayed a characteristic of propagation toward China. A detailed EKE budget revealed that $-\boldsymbol{V}'\cdot\nabla\phi'$ contained the major source of energy centers on the downstream of the Middle East trough and upstream of the western Pacific trough from 25 to 28 January 2008. The magnitudes of the energy conversion terms, $-\boldsymbol{V}_2'\cdot(\boldsymbol{V}'\cdot\nabla\overline{V_2})$ and $-\omega'\alpha'$, were too small to explain the development of the energy centers and jet streaks. The energy centers obtained energy at their entrance region and lost at their exit region by ageostrophic geopotential fluxes. There were four source regions of the flux: upstream, downstream, midlatitudes, and tropics. At the entrance region, the fluxes converged, increasing the geopotential gradient, which generated a stronger geostrophic wind and higher kinetic energy, resulting in an ascending motion

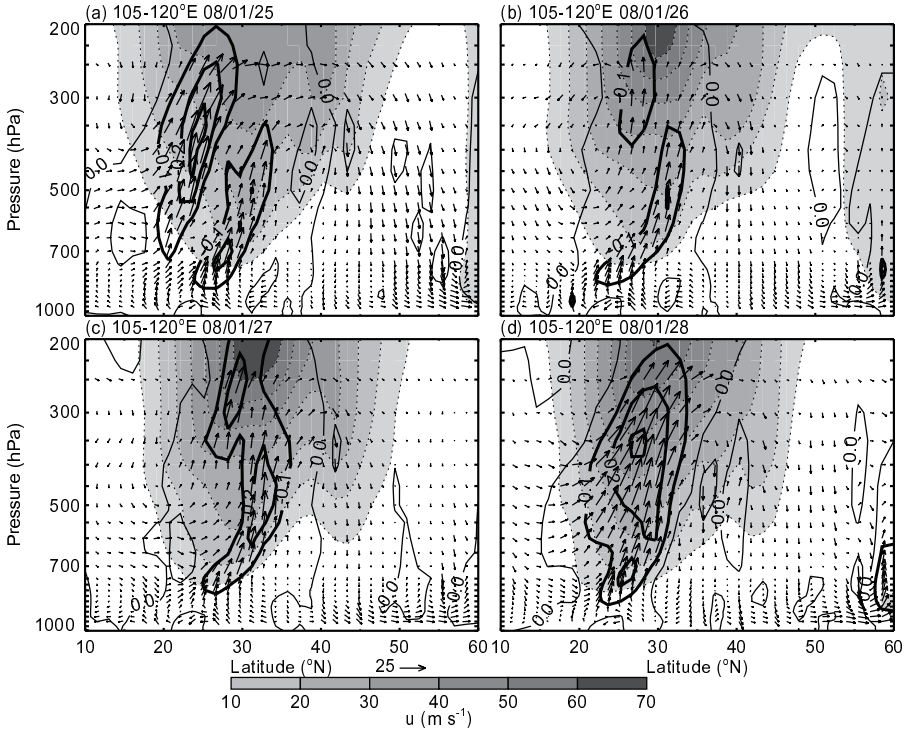

Fig. 10. Latitude–height cross sections of vertical velocity (thick solid lines: negative; thick dotted lines: positive, interval is 0.1 Pa s^{-1}), zonal wind (shadow, interval: 10 m s^{-1}), and ageostrophic wind flux vectors (the vertical component was multiplied by 100, unit vector: 25) averaged from 105° to 120°E from 25 to 28 January 2008.

which intensified the snowstorms over central and southern China.

Acknowledgements. The authors are grateful to the ECMWF for making their respective datasets readily available online. This work was supported by the National Basic Research Project of China (Grant Nos. 2013CB430105 and 2012CB417201), the National Natural Science Foundation of China (Grant No. 40930950), the Chinese Academy of Meteorological Sciences State Key Laboratory of Severe Weather (LaSW) (Grant No. 2011LASW-A01), and the Key Research Program of the Sciences (Grant No. KZZD-EW-05-01).

REFERENCES

Bluestein, H. B., 1993: *Synoptic-Dynamic Meteorology in Midlatitudes.* Volume II, *Observations and Theory of Weather Systems*. Oxford University Press, 594 pp.

Crochet, M., F. Cuq, F. M. Ralph, and S. V. Venkateswaran, 1990: Clear-air radar observations of the great October storm of 1987. *Dyn. Atmos. Oceans*, **14**, 443–461.

Danielsen, E. F., 1974: The relationship between severe weather, major dust storms and rapid cyclogenesis. *Synoptic Extratropical Weather Systems*, M. Shapiro, Ed., NCAR, Boulder, Colo., 215–241.

Danielson, R. E., J. R. Gyakum, D. N. Straub, 2006: A case study of downstream baroclinic development over the North Pacific Ocean. Part II: Diagnoses of eddy energy and wave activity. *Mon. Wea. Rev.*, **134**, 1549–1567.

Junker, N. W., R. E. Bell, and R. H. Grumm, 1990: Development, maintenance and strengthening of a cyclonic circulation system by coupled jets. *Conference of Severe Local Storms*. Amer. Meteor. Soc., Alberta, Canada, 450–454.

Ludlam, F. H., 1963: Severe local storms: A review. *Meteor. Monogr.*, No. 27, Amer. Meteor. Soc., 1–30.

Murakami, S., 2011: Atmospheric local energetics and energy interactions between mean and eddy fields. Part I: Theory. *J. Atmos. Sci*., **68**, 760–768.

Newton, C. W., 1963: Dynamics of severe convective storms. *Meteor. Monogr.*, No. 27, Amer. Meteor. Soc., 33–55.

Newton, C. W., 1967: Severe convective storms. Vol. 12, *Advances in Geophysics*, Academic Press, 257–303.

Orlanski, I., and J. Katzfey, 1991: The life cycle of a cyclone wave in the Southern Hemisphere. Part I: Eddy energy budget. *J. Atmos. Sci.*, **48**, 1972–1998.

Orlanski, I., and J. P. Sheldon, 1995: Stages in the energetics of baroclinic systems. *Tellus*, **47**, 605–628.

Palmén, E., and C. W. Newton, 1969: *Atmospheric Circulation Systems: Their Structural and Physical Interpretation*. Academic Press, 606 pp.

Petterssen, S., 1956: *Weather Analysis and Forecasting*. Vol. 2. McGraw-Hill, 191–195.

Reiter, E. R., 1963: *Jet-stream Meteorology*. The University of Chicago Press, 515 pp.

Shi, X. H, X. D. Xu, and C. G. Lu, 2010: The dynamic and thermodynamic structures associated with a series of heavy precipitation events over China during January 2008. *Wea. Forecasting*, **25**, 1124–1141.

Simmons, A., S. Uppala, D. Dee, and S. Kobayashi, 2007: ERA-

Interim: New ECMWF reanalysis products from 1989 onwards. Newsletter 110-Winter 2006/07, ECMWF, 11 pp.

Sun, J. H., and S. X. Zhao, 2010: The impacts of multiscale weather systems on freezing rain and snowstorms over Southern China. *Wea. Forecasting*, **25**, 388–407.

Takaya, K., and H. Nakamura, 2001: A formulation of a phase-independent wave-activity flux for stationary and migratory quasigeostrophic eddies on a zonally varying basic flow. *J. Atmos. Sci.*, **58**, 608–627.

Uccellini, L. W., and D. R. Johnson, 1979: The coupling of upper and lower tropospheric jet streaks and implications for the development of severe convective storms. *Mon. Wea. Rev.*, **107**, 682–703.

Uccellini, L. W., and P. J. Kocin, 1987: The interaction of jet streak circulations during heavy snow events along the east coast of the United States. *Wea. Forecasting*, **2**, 289–308.

Velden, C. S., and G. A. Mills, 1990: Diagnosis of upper-level processes influencing an unusually intense extratropical cyclone over Southeast Australia. *Wea. Forecasting*, **5**, 449–482.

Wen, M., S. Yang, A. Kumar, and P. Q. Zhang, 2009: An analysis of the large-scale climate anomalies associated with the snowstorms affecting China in January 2008. *Mon. Wea. Rev.*, **137**, 1111–1131.

Zhou, W., J. C. L. Chan, W. Chen, J. Ling, J. G. Pinto, and Y. P. Shao, 2009: Synoptic-scale controls of persistent low temperature and icy weather over Southern China in January 2008. *Mon. Wea. Rev.*, **137**, 3978–3991.

Zuo, Q. J., S. T. Gao, and D. R. Lü, 2013: The propagation of wave packets and its relationship with the subtropical jet over Southern China in January 2008. *Adv. Atmos. Sci.*, **30**, 67–76, doi: 10.1007/s00376-012-1197-6.